eprints@whiterose.ac.uk
https://eprints.whiterose.ac.uk/

LETTER • OPEN ACCESS

Farmers' first rain: investigating dry season rainfall characteristics in the Peruvian Andes

View the article online for updates and enhancements.

Environmental Research Communications

LETTER

Farmers' first rain: investigating dry season rainfall characteristics in the Peruvian Andes

Cornelia Klein[1,2] , **Emily R Potter**[1] , **Cornelia Zauner**[1], **Wolfgang Gurgiser**[1] , **Rolando Cruz Encarnación**[3] , **Alejo Cochachín Rapre**[3] and **Fabien Maussion**[1]

[1] Department of Atmospheric and Cryospheric Sciences, University of Innsbruck, Innsbruck, Austria
[2] UK Centre for Ecology and Hydrology, Wallingford, United Kingdom
[3] Autoridad Nacional del Agua, Unidad de Glaciología y Recursos HÍdricos, Huaraz, Peru

E-mail: conkle@ceh.ac.uk

Abstract

In the Peruvian Andes, the first light rainfalls towards the end of the dry season in August-September are known as *pushpa*. Softening soils and improving sowing conditions, these rains are crucial for planting dates and agricultural planning. Yet *pushpa* remains to date unexplored in the literature. This study uses observations and convection-permitting model simulations to describe the characteristics of *pushpa* in the Rio Santa valley (Peru). Comparing an observed *pushpa* case in August 2018 with a dry and wet event of the same season, we find *pushpa* to coincide with upper-level westerly winds that are otherwise characteristic for dry periods. These conditions impose an upper-level dry layer that favours small-scale, vertically-capped convection, explaining the low rainfall intensities that are reportedly typical for *pushpa*. Climatologically, we find 83% of *pushpa*-type events to occur under westerly winds, dominating in August, when 60% of the modelled spatial rainfall extent is linked to *pushpa*. Larger, more intense deep-convective events gradually increase alongside more easterly winds in September, causing the relative *pushpa* cloud coverage to drop tõ 20%. We note high inter-annual and -decadal variability in this balance between pushpa and intense convective rainfall types, with the spatial extent of pushpa rainfall being twice as high during 2000-2009 than for the 2010-2018 decade over the key sowing period. This result may explain farmers' perception in the Rio Santa valley, who recently reported increased challenges due to delayed but more intense *pushpa* rains before the rainy season start. We thus conclude that the sowing and germination season is crucially affected by the balance of *pushpa*-type and deep-convective rain, resulting in a higher probability for late first rains to be more intense.

1. Introduction

In the central tropical Andes, rain-fed farming practices are dictated by the strong rainfall seasonality that comes with the South American monsoon system, whose south-north progression produces pronounced wet and dry seasons (e.g. Vera *et al* 2006, Marengo *et al* 2012). This progression is linked to well-known large-scale circulation changes. Over the dry season, upper-level westerly winds dominate, transporting stable air masses from the Pacific towards the Andes with its core season from June to August. This regime shifts to easterly winds over the November - March core wet season, bringing with it moister, unstable air masses from the Amazon basin (Garreaud and Aceituno 2001, Garreaud 2009). The dry and wet regimes are linked by a pronounced transition period of a highly variable rainy season onset period, and a more gradual rainfall retreat with little variability (Giráldez *et al* 2020, Hänchen *et al* 2022). The focus region of this study is the Rio Santa valley in the Peruvian Andes (figure 1(a)), which is framed by the mountain ranges Cordillera Negra (>5000 m asl.) in the west and Cordillera Blanca to the east (>6000 m asl.), and counts more than 120,000 inhabitants within the

Figure 1. (a) Map of the WRF-CASE domain setup. D1 covers Peru and D2 the Rio Santa region (black outline). Coloured contours show the topography height. (b) Average precipitation timeseries (mm day^{-1}) in 2018 from a cross-valley transect of six rain gauges as shown in (h). The pushpa (17th August), DRY (6th September) and WET (20th November) events are marked as magenta, blue and green dashed lines, with the black dotted line indicating 1st November as climatological wet season start. (c), (f), (i) Satellite images of cloud cover in the pushpa, DRY and WET case respectively. (d), (g), (j) Top of the atmosphere brightness temperature (cloud top temperature, °C) at 16:00 LT for the pushpa, DRY and WET case respectively. (e), (h), (k) Precipitation daily totals (over 1 mm) for WRF-CASE in the pushpa, DRY and WET event, respectively. The coloured contours show the daily precipitation from the reference run (1200 UTC initialisation), with blue contours outlining where all ensemble members produce >1 mm day^{-1}. Note different value ranges for (e), (h) and (k). (e) also shows the latitude of the cross sections shown in figure 2.

larger agglomeration of its major city Huaraz (3052m asl.). Here, the wet season on which the predominantly rain-fed agriculture of the region relies, begins between mid-September and October and ends around May to early June (Giráldez *et al* 2020, Gurgiser *et al* 2016).

Before the core wet season however, and towards the end of the dry season, a period of reportedly small-scale lighter rains mark the start of the sowing season for the valley's farmers; dry season rains which are of such vital

importance that they are welcomed with festivities and carry the ancient Quechua name '*pushpa*' (Gurgiser *et al* 2016), forming part of local weather knowledge and proverbs, for example:

- Esteban MC Mendoza, Comunidad de Shupluy, Yungay: '*To forecast the weather my father said: If 'la pushpa' (first rains) appears, the poor fox will not eat any sheep and it will be a good year. If 'la pushpa' does not appear, the fox will begin to howl and eat sheep and it will be a bad year.*' (Gutiérrez 2008).

- Focal group in the Comunidad de Yanama, Yungay: '*There are people who forecast the weather of the year. They see it in August when the first rains fall. If 'la pushpa' is good, this means that it will be a good year.*' (Gutiérrez 2008).

- Focal group in Rio Santa valley: '*The climate has changed a lot, the rains. Before, the rains fell approximately on August 3 and those first rains were the 'pushpa', then they [the rains] left and returned in November.*' (Valverde 2012).

Local reports imply that the lighter nature of these early rains is crucial to preparing soils for sowing, softening them and limiting the level of erosion caused by heavier rainfall events associated with the rainy season (Gurgiser *et al* 2016). While the *pushpa* terminology is predominantly known throughout the Rio Santa valley, the importance of early rains for agriculture has been noted for other Andean regions, such as the semi-arid Altiplano in Bolivia (e.g. Valdivia *et al* 2013, Meldrum *et al* 2018). Yet, our physical understanding on the type and driving conditions of these dry season rainfall events is to date limited to what we can infer from local knowledge and personal communication. Furthermore, farmers' perceptions of trends, in particular of decreasing frequency and later onset of *pushpa* rains with adverse effects on crop growth, has yet to be corroborated. In that context and by analysing rain gauge data in the Rio Santa valley, Gurgiser *et al* (2016) conceded that the *in situ* data basis was too sparse and unreliable for light localised rains to make robust statements on potential *pushpa* trends. Similarly, available gridded rainfall datasets retrieved from remote sensing remain relatively coarse-scale (0.05°) for the detection of rainfall events, with expected biases in the low intensity range and questionable consistency for small-scale trend analyses (Mourre *et al* 2016, Hänchen *et al* 2022).

Thus, major difficulties for improving our understanding of *pushpa* events lie firstly in the lack of a data-based definition of these rains and secondly in their presumably light and small-scale nature with occurrence in complex topography, which limits our ability to directly observe and measure them. The aim of this study is therefore to help close this knowledge gap by evaluating the characteristics and local atmospheric drivers of an observed and locally confirmed *pushpa* event that occurred during field work in the Rio Santa valley on the 17 August 2018. To obtain the needed atmospheric data, we employ the Weather Research and Forecasting (WRF) model to reproduce the event at 2km spatial resolution in a convection-permitting ensemble forecasting setup. Based on this representative event, our study proposes a first data-based definition for *pushpa* rain by comparing its distinct environmental conditions to a typical dry and wet event of the same season. In a second step, we exploit an existing climatological 4 km WRF dataset produced for the Rio Santa valley (in review, Potter *et al* 2023). It provides temporally-consistent decadal atmospheric and rainfall data, allowing us to quantify *pushpa* frequency and potential trends therein over the last 39 years (1980-2018).

2. Datasets and methods

2.1. Observational datasets
To verify the observed *pushpa* rainfall case and for the identification of a dry and wet event for comparison, we use hourly *in situ* rainfall measurements along a transect in the Rio Santa valley using 6 rain gauges at altitudes ranging between 3084 m and 3996 m, which have been collecting data since 2017 (c.f. figures 1(a), (h), https://agroclim-huaraz.info/live/). To compare afternoon (local time, LT) cloud cover patterns, we also show MODIS Aqua visible cloud cover (1330LT, https://lpdaac.usgs.gov) and 1600~LT GRIDSAT-B1 thermal-infrared cloud top temperatures (Knapp *et al* 2011) for the three case study days.

2.2. Selection of pushpa, dry and wet events
In-situ rainfall measurements are shown for August to November 2018 in figure 1(b), which covers the transition period from dry to rainy season conditions in the Rio Santa valley. On the 17th August, the rain gauges recorded light rainfall along the measurement transect, in line with on-site observations and its characterisation as '*pushpa* event day' by local partners (magenta vertical line, *pushpa*). We further identified a dry and wet event situation within the same period to compare to the *pushpa* day. These events were chosen under the condition that they occurred within multi-day dry and wet spells, and with the dry event (red line, DRY) occurring after the

pushpa day. This evaluation follows the assumption that the *pushpa* rains tend to precede subsequently returning dry conditions, and are expected in the dry season with first occurrence in August. The wet event on the other hand is chosen to represent a situation after the rainy season is established (blue line, WET), characterised in figure 1(b) by increasing frequency of intense rainfall events over October-November. We thus evaluate a mid-August *pushpa* event against an early-September DRY case, and an end-of-November WET case, covering the transition period from dry to rainy season.

2.3. WRF simulations

The Advanced Research core (ARW) WRF Model v4.0 (Skamarock *et al* 2021) was run with a 2 km convection-permitting (cumulus parameterisation switched off) domain centred on the Rio Santa basin (D2), which was nested within a Peru-encompassing parent domain at 10 km horizontal resolution (D1) with parameterised convection (figure 1(a)). D1 was forced by the ERA5 reanalysis (Hersbach *et al* 2020) without nudging. Except for convection treatment, both domains used the same parameterisation setup as detailed in supplementary table 1. Here, we only analyse hourly output from the nested 2 km domain. We performed 2-day experiments for each of the case study days, where the first day is initialised at 1200LT and discarded to allow for model spin-up. In the same fashion, two further 2-day simulations were run with perturbed initial conditions (starting time at -6 and +6 hours from reference simulation), to account for internal model variability. We use the 3-member ensemble for each of the case study days to illustrate event representation consistency. However, if not otherwise indicated, all detailed process analyses are done for the 1200 LT reference simulation only.

In addition, for climatological assessment of our case study findings, we use a previously published convection-permitting WRF dataset for the region (Potter *et al* 2023), which covers 1980-2018 at 4 km horizontal resolution. The WRF setups between our case studies (henceforth WRF-CASE) and this climatological simulation (WRF-CLIM) differ, adding robustness to process-based findings that are represented in both datasets.

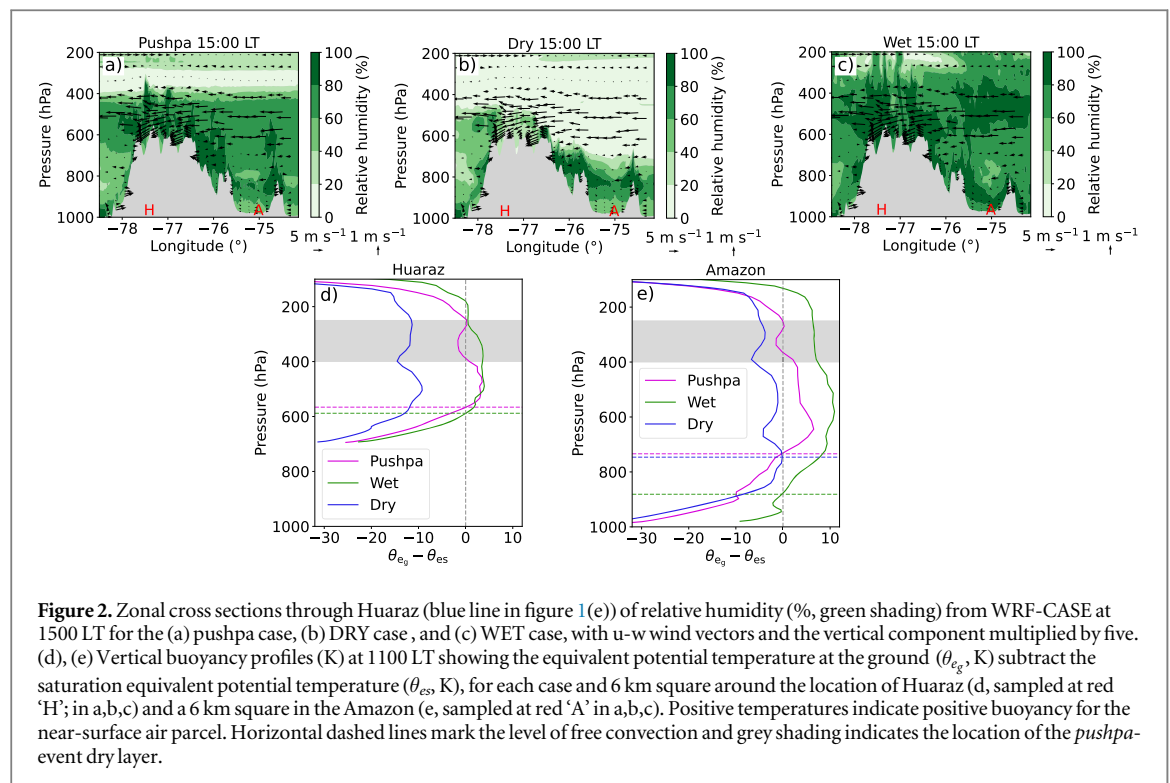## 3. Observed and modelled convection patterns

Examining the large-scale cloud cover for the *pushpa*, DRY and WET event in MODIS observations, we note that clouds are smaller-scale and scattered on the *pushpa* day with cloud patterns visibly following topographic features (figure 1(c)). On the other hand, the WET event exhibits a closed cloud deck from the Amazon out to the Pacific in the west (figure 1(i)), while in the DRY case the Andes stay cloud-free (figure 1(f)). GRIDSAT cloud top temperatures (CTTs, figure 1(d)) further demonstrate that convection stays shallower on the *pushpa* day with CTTs largely $\geqslant -25\ °C$, including over the Rio Santa valley, while the WET case exhibits widespread deep clouds $\leqslant -40\ °C$ (figure 1(j)).

Finally, we find that WRF-CASE is able to capture these differences between events (figure 1(e)), most notably the structural differences in convection between the scattered, lighter *pushpa* rainfall and wide-spread, intense WET case rainfall patterns, while the DRY case shows zero rain. These differences in rainfall intensities and patterns are consistent across the three-member WRF-CASE ensemble (blue contour, figure 1(e)), suggesting that the large-scale atmospheric situation has a strong control on the convection characteristics for the three cases.

4. Pushpa case study versus dry and wet environments

4.1. Large-scale circulation and convective environments

Using the reference WRF-CASE ensemble member, figures 2(a)–(c) shows cross-sections of modelled circulations and relative humidity (RH) along a transect through the city of Huaraz in the Rio Santa valley at 1500LT, when rainfall occurred for the *pushpa* and WET case (c.f. supplementary figure 1). It is evident that the atmosphere is considerably drier on a large scale for the DRY case, with RH $\geqslant 60\%$ confined to below ~ 700 hPa to the east of the Andes, in the Amazon basin (figure 2(b)). On the other hand, the WET case features widespread RH values $\geqslant 60\%$ over the entire atmospheric column (figure 2(c)). In addition, convective updraughts (RH $\geqslant 80\%$) are evident over the Andes crest, which reach up to ~ 200 hPa. For the *pushpa* case, we find low- and mid-level RH to be more similar to the WET than to the DRY case ($\geqslant 60\%$, figure 2(a)). However, above ~ 400 hPa, a distinct dry layer (RH $\leqslant 20\%$) spans the entire region and large-scale upper-level westerly winds prevail, which resembles upper-level DRY case conditions. Furthermore, *pushpa* updraughts remain shallower, not fully penetrating the dry layer. We thus identify mixed conditions on the *pushpa* day, with enhanced moisture at low- and mid-levels closer to WET conditions, while levels >400 hPa are still controlled by dry westerly winds from the Pacific. These are characteristic for dry season conditions and still prevail during the DRY case, while they switch to upper-level easterly winds when the rainy season is established, as visible for the WET case.

Figure 2. Zonal cross sections through Huaraz (blue line in figure 1(e)) of relative humidity (%, green shading) from WRF-CASE at 1500 LT for the (a) pushpa case, (b) DRY case , and (c) WET case, with u-w wind vectors and the vertical component multiplied by five. (d), (e) Vertical buoyancy profiles (K) at 1100 LT showing the equivalent potential temperature at the ground (θ_{e_g}, K) subtract the saturation equivalent potential temperature (θ_{es}, K), for each case and 6 km square around the location of Huaraz (d, sampled at red 'H'; in a,b,c) and a 6 km square in the Amazon (e, sampled at red 'A' in a,b,c). Positive temperatures indicate positive buoyancy for the near-surface air parcel. Horizontal dashed lines mark the level of free convection and grey shading indicates the location of the *pushpa*-event dry layer.
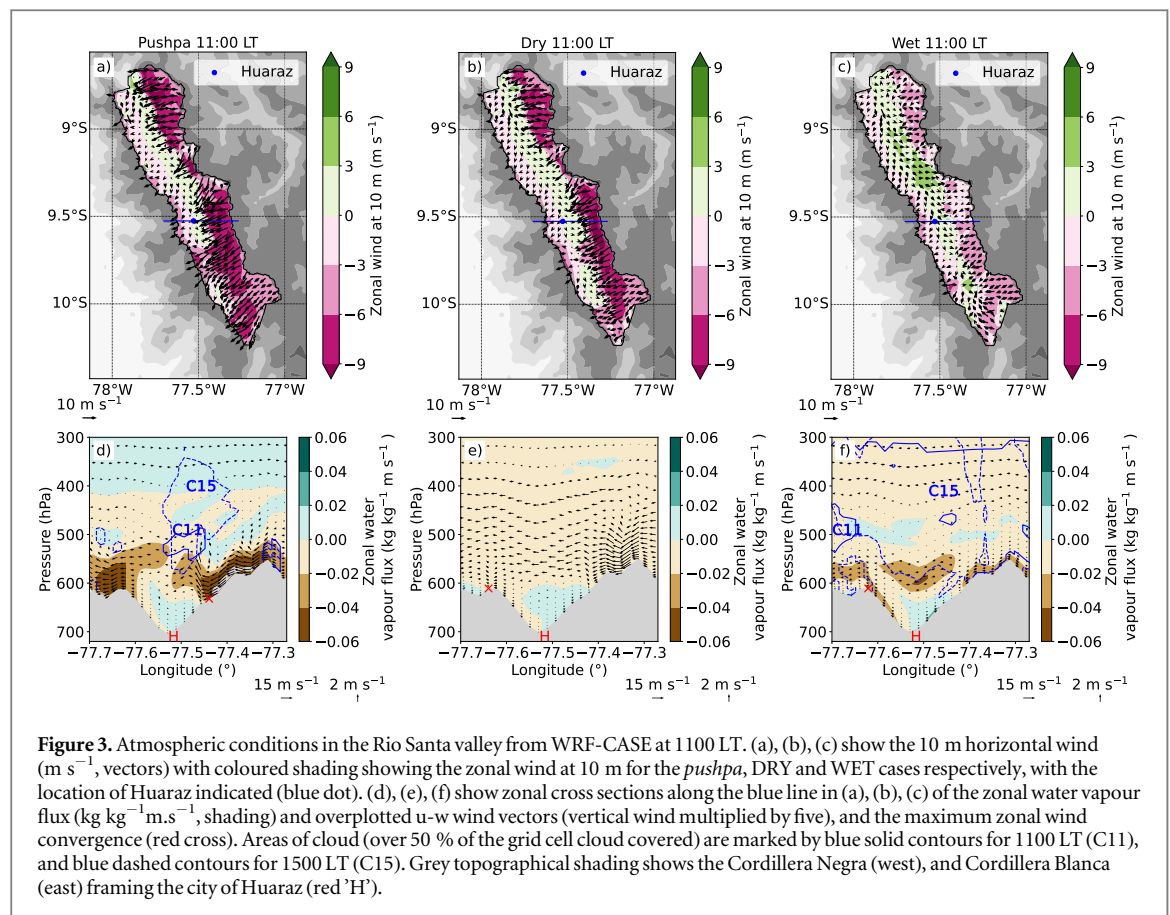
Exploring pre-convective environments (1100LT) in the Rio Santa valley centred on Huaraz (sampled at 'H' at 3052m asl. in figures 2(a)–(c)), we note that the *pushpa* and WET cases show strong similarities in the buoyancy profile (figure 2(d)) with comparable low-lying level of free convection (LFC, dashed horizontal lines) and positive buoyancy between 600-400hPa, indicating potential for convection. However, while positive buoyancy reaches above 200 hPa for the WET case, neutral buoyancy is already reached close to 400 hPa in the *pushpa* case, aligned with the location of the marked dry layer (figure 2(d), grey shading). This indicates that the dry layer is indeed limiting deep convection on the *pushpa* day. For the DRY case, buoyancy remains negative throughout the profile.

To understand whether these pre-convective environments are representative at a larger scale and at lower altitude, we compare the conditions in the elevated Rio Santa valley to vertical profiles at the same latitude but 2.5° to the east in the Amazon lowlands ('A' at 200 m altitude in figures 2(a)–(c)). In contrast to the conditions around Huaraz (figure 2(d)), we find the *pushpa* conditions here to be closer to DRY than to WET conditions in the low-levels (985-800 hPa, figure 2(e)). The LFC is situated at ~750 hPa, about 2.3km above ground, making this instability unlikely to be released without significant orographic lifting. This is also reflected in figure 2(a), where high-RH convective updraughts are confined to topographic features. Similar to the Rio Santa, *pushpa* day buoyancy becomes negative in the upper-level dry layer, while the WET case convection is not capped.

This shows that in the model, atmospheric conditions in the *pushpa* case are not favourable for convection and rainfall production on the large scale, as is the case for the WET event, but seems to depend on local conditions over topography. Furthermore, we find the distinct upper-level dry layer to be the major difference between the *pushpa* and WET convective environments. The dry layer limits the vertical expansion of deep convection, explaining warmer cloud top temperatures compared to WET (figures 1(c), (f)). It thus seems likely that in addition to lower specific humidity, the dilution of moist convective updraughts by dry air entrainment (e.g. James and Markowski 2010, Ahmed and Neelin 2021) contributes to the low rainfall intensities that are reportedly characteristic for *pushpa* events.

4.2. Valley-scale conditions and event initiation

We now inspect the local conditions that created the *pushpa* event in the Rio Santa valley as represented in the WRF-CASE simulations. The pre-convective (1100LT) 10 m wind fields show similar patterns for the *pushpa* and DRY events (figures 3(a), (b)), with strong easterly winds penetrating into the valley over the Cordillera Blanca crest. Cross-sections through Huaraz (H) in figures 3(d), (e) reveal that this wind is associated with an increased mid-level moisture flux, reaching down the eastern slope to create a convergence line with the up-valley winds. In WRF-CASE, the *pushpa* event was triggered along this line, as indicated by cloud cover (blue solid contours at 1100LT, C11), and subsequently grew into a localised convective storm with limited vertical extent (dashed blue line at 1500LT, C15). In comparison, valley-scale convergence and moisture influx are

Figure 3. Atmospheric conditions in the Rio Santa valley from WRF-CASE at 1100 LT. (a), (b), (c) show the 10 m horizontal wind (m s^{-1}, vectors) with coloured shading showing the zonal wind at 10 m for the *pushpa*, DRY and WET cases respectively, with the location of Huaraz indicated (blue dot). (d), (e), (f) show zonal cross sections along the blue line in (a), (b), (c) of the zonal water vapour flux (kg kg^{-1}m.s^{-1}, shading) and overplotted u-w wind vectors (vertical wind multiplied by five), and the maximum zonal wind convergence (red cross). Areas of cloud (over 50 % of the grid cell cloud covered) are marked by blue solid contours for 1100 LT (C11), and blue dashed contours for 1500 LT (C15). Grey topographical shading shows the Cordillera Negra (west), and Cordillera Blanca (east) framing the city of Huaraz (red 'H').

weaker in the WET case (figures 3(f)), with large-scale deep convection entering from the east and covering the entire valley by 1500LT (blue dashed contours, C15), reaching over 300 hPa.

Given we find stronger down-slope easterly winds for the pushpa and DRY conditions than for the WET event, we conclude that these winds are more characteristic for the dry season in the Rio Santa valley. Our results further suggest that these winds may be instrumental in triggering local pushpa convection, as illustrated by the modelled pushpa event. The cloud cover extent found here confirms the localised, small scale of *pushpa* in comparison to the large-scale rainfall conditions associated with the WET case.
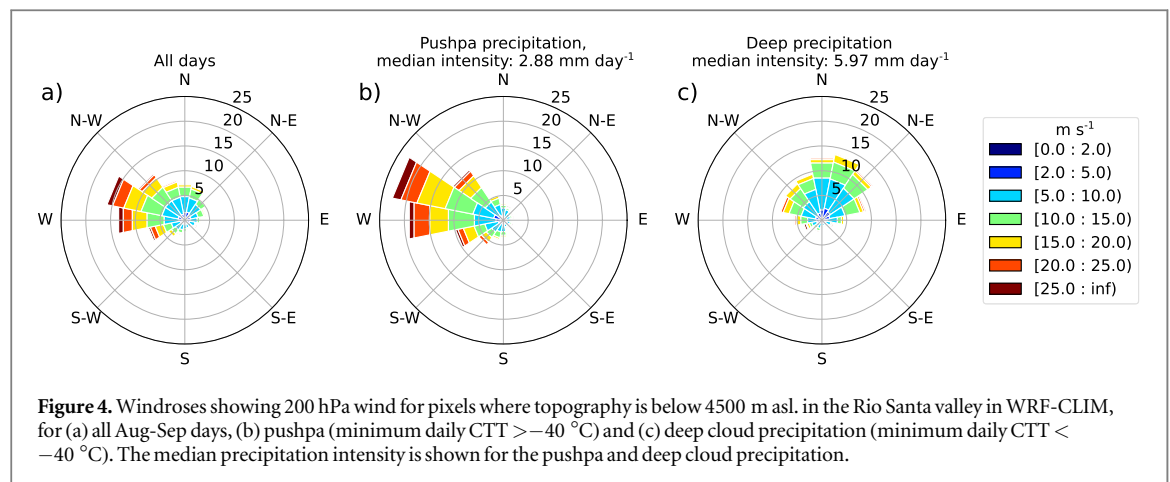
5. Climatological pushpa frequency in the Rio Santa valley

5.1. Data-based definition of *pushpa*

Based on the above case-study results, we propose that *pushpa*-type events are rainfall events that are capped by an upper-level dry layer (400-250 hPa, c.f. figure 2(a)), where the layer is maintained by large-scale dry season circulation characteristics, i.e. occurring as a consequence of dominant upper-level westerly winds. Assuming *pushpa* characteristics are crucially defined by its inability to fully penetrate this layer, we use daily minimum CTTs from WRF-CLIM as indicator to separate *pushpa*-type (CTT < -40 °C) and deep-type (CTT < -40 °C) precipitation events per day and pixel (> 1 mm day^{-1}). Here, the threshold of -40 °C corresponds to the average atmospheric temperature at the upper level of the case-study dry layer (250 hPa, c.f. supplementary figure 2), thus controlling for the condition that *pushpa*-type clouds do not grow beyond the layer. Note that we refer to this definition as '*pushpa*-type' events, as (1) the *pushpa* terminology traditionally refers specifically to the locally and subjectively identified first occurrences of these rains in the year (as in the case-study, usually in August), and (2) our data-based definition cannot control for the agriculturally-important effects on the ground that would define a 'real' *pushpa*.

We apply this -40 °C CTT separation of *pushpa*-type and deep clouds to the 39 years of August to September periods in WRF-CLIM on a per-pixel basis. For this, we exclude regions above 4500 m asl. to focus on agriculturally relevant parts of the Rio Santa valley. The resulting *pushpa*-type classification shows a pronounced upper dry layer, corresponding to the *pushpa* case-study findings in WRF-CASE (supplementary figure 2). Figure 4(a) illustrates that over the considered period, average upper-level winds at 200 hPa are predominantly (north-)westerly (69% of total), in line with expected dry season conditions. However, the (north)-westerly wind

Figure 4. Windroses showing 200 hPa wind for pixels where topography is below 4500 m asl. in the Rio Santa valley in WRF-CLIM, for (a) all Aug-Sep days, (b) pushpa (minimum daily CTT > −40 °C) and (c) deep cloud precipitation (minimum daily CTT < −40 °C). The median precipitation intensity is shown for the pushpa and deep cloud precipitation.

fraction further increases to 83% when only considering *pushpa*-type rainfall pixels (figure 4(b)), confirming that a large majority occur under upper-level westerly wind influence. On the other hand, we find a preference for deep rainfall pixels to coincide with times when the upper-level flow switches to light northerlies/north-easterlies or when the westerly flow is weakened (figure 4(c)).

The marked difference in upper-level wind direction between *pushpa*-type and deep rainfall events strongly suggests a dominant control of large-scale favourable conditions to allow deep events, while the upper-levels are hostile for convection on *pushpa*-type days, mostly allowing locally-triggered scattered rain. Accordingly, median *pushpa*-type rainfall intensities in WRF-CLIM are lower (3 mm day^{-1}) than deep rainfall intensities (6 mm day^{-1}) (figures 4(b), (c)), with lower CTTs i.e. higher cloud tops being associated with more intense rain (supplementary figure 3).
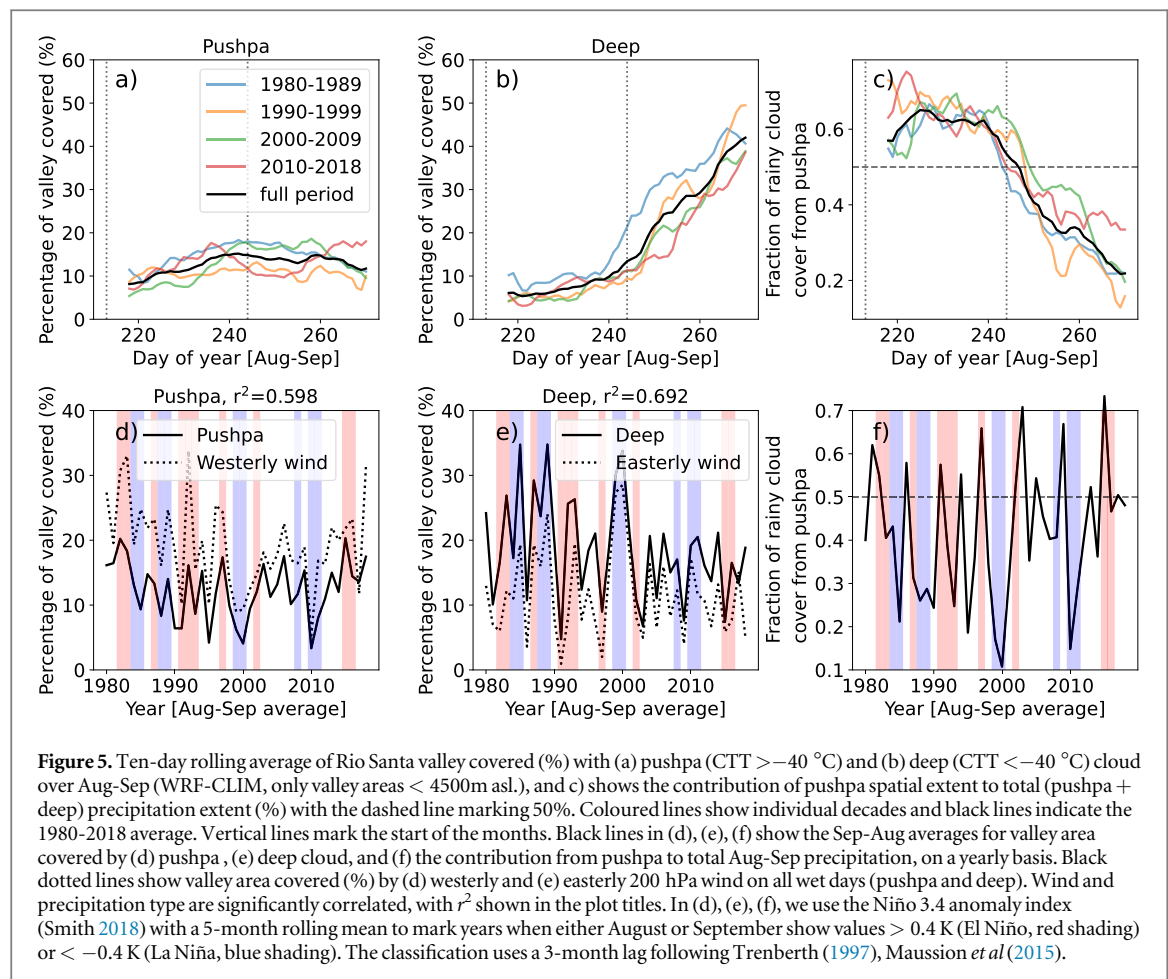
5.2. Balance of pushpa-type and deep rainfall events

We are now investigating the balance between *pushpa*-type and deep events for the dry-to-wet transition season over August and September (Aug-Sep) in WRF-CLIM. Figure 5(a) illustrates the 10-day centred-average (over 39 years) spatial extent of rainy cloud cover for *pushpa*-type events in the Rio Santa valley, which gradually increases over August and remains relatively constant on a small scale with around 10% of the valley covered through September. On the other hand, deep events are less frequent over August, but increase sharply in September, reaching over 40% daily coverage in the valley (figure 5(b)). The dominant contribution to rainy cloud cover thus shifts from dominant small-scale *pushpa*-type in August to dominant wider-spread deep precipitation in September (figure 5(c)), suggesting a gradual transition from low to high intensity precipitation events as the rainy season approaches. Interestingly, this is not accompanied by a decrease in *pushpa*-type cloud cover, but predominantly linked to the gradual increase in deep cloud cover.

Comparing individual decades (coloured lines, figure 5(c)), there is no evident shift in the balance of *pushpa*/ deep cloud cover over the different decades. However, the spatial extent of *pushpa* from end-August to mid-September for most recent years (2010-2018) was about half of the extent seen for 2000-2009; a large change during the key sowing period that may explain some of the recently perceived increased difficulties by farmers that they link to delayed and too intense *pushpa* rains (Gurgiser *et al* 2016). Indeed, we find the Aug-Sep balance between *pushpa*-type and deep cloud cover to be highly variable from year to year (Figures 5(d), (e)), but indicating no trend in either *pushpa* cloud cover, *pushpa* contribution to total rainy cloud cover (figure 5(f)) or *pushpa* intensity (supplementary figure 4). However, we do see a strong link of inter-annual rainfall-type variability to upper-level wind conditions, with the spatial extent of westerly wind explaining about 60% of the *pushpa* cloud cover variability (red line, figure 5(d)), while valley area covered by easterly wind explains about 70% of the deep cloud cover variability in the Rio Santa valley (red line, figure 5(e)). The variability shows some alignment with the El Niño Southern Oscillation, where westerly wind and pushpa tend to show higher coverage during El Niño than La Niña years (red and blue shading, figures 5(d), (f)). These findings support our hypothesis that upper-level westerly winds are an important pre-condition for *pushpa* rainfall by helping to maintain the capping upper-level dry layer, while deep clouds and rain strongly depend on easterly wind conditions.

6. Discussion and conclusion

The aim of this study was to explore the characteristics of dry season *pushpa* rainfall and its driving atmospheric conditions, based on a confirmed *pushpa* event in 2018 and high-resolution WRF simulations for the Rio Santa

Figure 5. Ten-day rolling average of Rio Santa valley covered (%) with (a) pushpa (CTT $> -40\ °C$) and (b) deep (CTT $< -40\ °C$) cloud over Aug-Sep (WRF-CLIM, only valley areas < 4500 m asl.), and c) shows the contribution of pushpa spatial extent to total (pushpa + deep) precipitation extent (%) with the dashed line marking 50%. Coloured lines show individual decades and black lines indicate the 1980-2018 average. Vertical lines mark the start of the months. Black lines in (d), (e), (f) show the Sep-Aug averages for valley area covered by (d) pushpa , (e) deep cloud, and (f) the contribution from pushpa to total Aug-Sep precipitation, on a yearly basis. Black dotted lines show valley area covered (%) by (d) westerly and (e) easterly 200 hPa wind on all wet days (pushpa and deep). Wind and precipitation type are significantly correlated, with r^2 shown in the plot titles. In (d), (e), (f), we use the Niño 3.4 anomaly index (Smith 2018) with a 5-month rolling mean to mark years when either August or September show values > 0.4 K (El Niño, red shading) or < -0.4 K (La Niña, blue shading). The classification uses a 3-month lag following Trenberth (1997), Maussion *et al* (2015).

valley in the Peruvian Andes. We used the confirmed *pushpa* case to establish a definition based on CTTs to distinguish *pushpa* rains from deeper, more intense rainfall types as are typical for the rainy season in the region. Both model datasets, WRF-CASE and WRF-CLIM, suggest *pushpa* rainfall to be a small-scale, localised rainfall type that preferentially occurs within the valley with moist mid-levels but under dry upper-level westerly wind conditions. These are accompanied by the presence of a 400–250 hPa upper-level dry layer, which limits the vertical extent of *pushpa* convection. Conversely, the more intense rainy season rainfall is more likely to occur with upper-level easterly wind introducing favourable conditions for convection on a large-scale, resulting in wider-spread rainfall beyond the valley, which we found to be twice as intense as *pushpa* rain in WRF-CLIM. This sets *pushpa* into context of previous findings based on ground-radar measurement campaigns in the Peruvian Andes, where an increase in convection vertical extent and rainfall intensity was detected going from the September-November to December-March peak rainfall season (Kumar *et al* 2020), with comparably very light rainfall detected in August (Seidel *et al* 2019).

Focusing on the Aug-Sep transition period before the rainy season, we find westerly upper-level winds explaining 60% of inter-annual variability in the valley area covered by *pushpa*. On the other hand, upper-level easterlies explain 70% of deep rainfall inter-annual variability, reflecting a rainfall enhancement under easterly winds previously found for the peak rainy season in the tropical Andes (Garreaud and Aceituno 2001, Thibeault *et al* 2012, Sulca *et al* 2016).

As such, our results are in line with local reports on the localised and light nature of *pushpa* rainfalls (c.f. Gurgiser *et al* 2016), where we identify strong indications for these characteristics to be controlled by the existence of an upper-level dry layer that is gradually moistened over the transition period to allow deeper convection and more intense rainfall. In WRF-CLIM, *pushpa* events dominate the spatial extent of rainy cloud cover in the Rio Santa valley in August, after which coverage from deeper, more intense convection increases steadily. From early September on, deeper convection shows higher valley coverage than *pushpa* as precursor for the rainy season, whose onset Giráldez *et al* (2020) place around late September for the central Peruvian Andes. Focusing on the Mantaro basin in the Peruvian Andes, Giráldez *et al* (2020) also note a later onset of the rainy season between 1965-2013, a trend that is however dominated by early-onset years before the 1980s. Using WRF-CLIM, we do not find a significant trend in the spatio-temporal frequency in either *pushpa* or deep rainfall-types that would indicate a change in rainy season onset conditions since the 1980s. Instead, there is a

high year-to-year variability in the balance between *pushpa* and deep intense rainfall, with *pushpa* contributing between 20% to 65% of the total rainy cloud cover in the Rio Santa valley in Aug-Sep and minimum coverage in La Niña years. Paired with this temporal variability, the relatively small spatial extent of *pushpa* events further increases the uncertainty for when first rains may fall at any location within the valley. Our results showing a continuous increase in the spatial extent of deep rainfall throughout Aug-Sep suggest that the later first rains occur at any location, the more likely these rains are to be more intense rather than *pushpa*-type. At the same time, we expect that if the large-scale conditions impose a late rainy season onset through prolonged upper-level westerly wind influence, the period for which *pushpa*-type rainfall dominates may become longer.

In conclusion, we illustrated that *pushpa* rainfall can be identified by its low vertical extent compared to typical rainy season rainfall. It is a transition season rainfall that can occur intermittently with more intense events over the Aug-Sep period. Our results indicate consistency with reports from the local population on *pushpa* characteristics, though it should be noted that our interpretation of *pushpa*-type rainfall here is broad and ultimately tied to relationships to atmospheric drivers. For locals in the Ancash region, only the first few witnessed rainfall events will be '*pushpa*', evoking linked beliefs on the subsequently favourable progression of the rainy season. It is likely that similar rainfall progression from light to heavy rainfall towards the rainy season may be acting and be of significance for the local population in other Andean regions, albeit with different terminologies. Our findings highlight the need to consider rainfall changes outside of peak rainy seasons, particularly in the climate change context, with more research needed for the variable dry-to-wet transition periods when small changes and high variability can have a big impact on agricultural planning.

Acknowledgments

Data availability statement

The data that support the findings of this study are openly available at the following URL/DOI: https://cluster.klima.uni-bremen.de/~fmaussion/share/wrf_puspa/. https://doi.org/10.5285/7F3E4CFC-B75B-4758-85FC-58634BD7B1D1.

Author contributions

CK, EP, CZ, WG and FM conceptualised the study, with input from RE and AR EP and CZ performed the simulations; CK, EP CZ and FM led on the methodological design. WG led the installation of HOBOs/AWS on site. Case study analyses were first conceived by CZ with input from FM and CK, while climatological analyses were performed by EP and CK. Final plots were created by EP, and CK led the writing of the manuscript with contributions from all authors.

ORCID iDs

Cornelia Klein ⓘ https://orcid.org/0000-0001-6686-0458
Emily R Potter ⓘ https://orcid.org/0000-0001-5273-1292
Wolfgang Gurgiser ⓘ https://orcid.org/0000-0003-1150-344X
Rolando Cruz Encarnación ⓘ https://orcid.org/0000-0001-7166-3053
Fabien Maussion ⓘ https://orcid.org/0000-0002-3211-506X

References

Ahmed F and Neelin J D 2021 Protected convection as a metric of dry air influence on precipitation *J. Clim.* **34** 3821–38
Garreaud R D 2009 The Andes climate and weather *Advances in Geosciences* **22** 3–11
Garreaud R D and Aceituno P 2001 Interannual rainfall variability over the South American Altiplano *J. Clim.* **14** 2779–89
Giráldez L, Silva Y, Zubieta R and Sulca J 2020 Change of the rainfall seasonality over central peruvian andes: Onset, end, duration and its relationship with large-scale atmospheric circulation *Climate* **8** 2–23

Gurgiser W, Juen I, Singer K, Neuburger M, Schauwecker S, Hofer M and Kaser G 2016 Comparing peasants' perceptions of precipitation change with precipitation records in the tropical Callejon de Huaylas, Peru *Earth System Dynamics* **7** 499–515

Gutiérrez R 2008 Papas nativas desafiando al cambio climático: Propuesta de adaptación tecnológica del cultivo de papas nativas frente al cambio climático en Cusco y Ancash *Soluciones Prácticas* **1** 6–83

Hänchen L, Klein C, Maussion F, Gurgiser W, Calanca P and Wohlfahrt G 2022 Widespread greening suggests increased dry-season plant water availability in the Rio Santa valley *Peruvian Andes Earth System Dynamics* **13** 595–611

Hersbach H *et al* 2020 The ERA5 global reanalysis *Q. J. R. Meteorolog. Soc.* **146** 1999–2049

James R P and Markowski P M 2010 A numerical investigation of the effects of dry air aloft on deep convection *Mon. Weather Rev.* **138** 140–61

Knapp K R *et al* 2011 Globally gridded satellite observations for climate studies *Bull. Am. Meteorol. Soc.* **92** 893–907

Kumar S *et al* 2020 Rainfall characteristics in the central Andes of Peru from a vertically pointed profile rain radar and in-situ field campaign *Atmosphere* **11** 1–39

Marengo J A *et al* 2012 Recent developments on the South American monsoon system *Int. J. Climatol.* **32** 1–21

Maussion F, Gurgiser W, Großhauser M, Kaser G and Marzeion B 2015 Enso in uence on surface energy and mass balance at shallap glacier, cordillera blanca, peru *The Cryosphere* **9** 1663–83

Meldrum G *et al* 2018 Climate change and crop diversity: farmers' perceptions and adaptation on the bolivian altiplano *Environment, Development and Sustainability* **20** 703– 730

Mourre L, Condom T, Junquas C, Lebel T, Sicart J E, Figueroa R and Cochachin A 2016 Spatio-temporal assessment of WRF, TRMM and in situ precipitation data in a tropical mountain environment *(Cordillera Blanca, Peru)* **20** 125–41

Potter E *et al* 2023 A future of extreme precipitation and droughts in the Peruvian Andes *npj Clim Atmos Sci* **6** 96

Seidel J *et al* 2019 Precipitation characteristics at two locations in the tropical andes by means of vertically pointing micro-rain radar observations *Remote Sensing* **11** 1–18

Skamarock C *et al* 2021 *A Description of the Advanced Research WRF Model Version 4.3* **No. NCAR/TN-556+STR** 1–300

Smith C 2018 Ni no 3.4 from NOAA ENSO anomaly dataset (https://psl.noaa.gov/gcoswgsp/Timeseries/Nino34/) (Accessed on 01,11, 2022)

Sulca J, Vuille M, Silva Y and Takahashi K 2016 Teleconnections between the peruvian central andes and northeast Brazil during extreme rainfall events in austral summer *Journal of Hydrometeorology* **17** 499–515

Thibeault J, Seth A and Wang G 2012 Mechanisms of summertime precipitation variability in the bolivian altiplano: Present and future *Int. J. Climatol.* **32** 2033–41

Trenberth K E 1997 The definition of el nino *Bull. Am. Meteorol. Soc.* **78** 2771–8

Valdivia C, Thibeault J, Gilles J L, García M and Seth A 2013 Climate trends and projections for the Andean Altiplano and strategies for adaptation *Advances in Geosciences* **33** 66–77

Valverde J 2012 Estudio de saberes locales sobre gestion callejón de huaylas - región ancash *Soluciones Prácticas* **1** 59

Vera C *et al* 2006 Toward a unified view of the American monsoon systems *J. Clim.* **19** 4977–5000